Available online at BCREC website: https://bcrec.id

Bulletin of Chemical Reaction Engineering & Catalysis, 17 (4) 2022, 743-754

Research Article

Effect of Precursor and Temperature Annealing on the Catalytic Activity of Intermetallic Ni_3Sn_2 Alloy

R. Rodiansono[1,2,*], Atina Sabila Azzahra[2], Sadang Husain[3], Pathur Razi Ansyah[4]

[1]Department of Chemistry, Lambung Mangkurat University, Jl. A. Yani Km 36, Banjarbaru 70714, Indonesia.
[2]Inorganic Materials and Catalysis (IMCat) Lab, Catalysis for Sustainable Energy & Environment (CATSuRe), Lambung Mangkurat University, Jl. A. Yani Km 36, Banjarbaru 70714, Indonesia.
[3]Department of Physics, Lambung Mangkurat University, Jl. A. Yani Km 36, Banjarbaru 70714, Indonesia.
[4]Department of Mechanical Engineering, Lambung Mangkurat University, Jl. A. Yani Km 35.5, Banjarbaru 70714, Indonesia.

Received: 21st September 2022; Revised: 30th October 2022; Accepted: 30th October 2022
Available online: 7th November 2022; Published regularly: December 2022

Abstract

The effect of nickel precursors and the temperature annealing to obtain intermetallic Ni_3Sn_2 alloy catalysts on its activity and selectivity in the selective hydrogenation of biomass-derived furfural (FFald) were investigated. Two types of nickel precursors (c.a., *i*) nickel metal (Ni°) derived from Raney®nickel and *ii*) nickel ion (Ni^{2+}) derived from nickel chloride) were employed as the starting materials via hydrothermal at 423 K for 24 h followed by reduction with H_2 at the elevated temperature of 573-873 K for 1.5 h. The physico-chemical properties of the intermetallic Ni_3Sn_2 were characterized by XRD, N_2-, and H_2-adsorption, ICP-AES, and NH_3-TPD. The intermetallic Ni_3Sn_2 alloy catalysts, both bulk and supported, demonstrated high activity and selectivity towards hydrogenation of FFald. The activity and selectivity of γ-Al_2O_3 and AA-supported Ni_3Sn_2 alloy catalysts in the hydrogenation of FFald to furfuryl alcohol (FFalc) were maintained even after annealing at up to 873 K, but that of bulk Ni_3Sn_2 drastically dropped. Ni-Sn alloy catalysts which were obtained from Raney®Ni precursor showed more stable than that of nickel salts during hydrogenation of furfural to furfuryl alcohol.

Keywords: intermetallic Ni_3Sn_2; bulk & supported Ni_3Sn_2; selective hydrogenation; furfural; furfuryl alcohol

How to Cite: R. Rodiansono, A.S. Azzahra, S. Husain, P.R. Ansyah (2022). Effect of Precursor and Temperature Annealing on the Catalytic Activity of Intermetallic Ni_3Sn_2 Alloy. *Bulletin of Chemical Reaction Engineering & Catalysis*, 17(4), 743-754 (doi: 10.9767/bcrec.17.4.15923.743-754)

Permalink/DOI: https://doi.org/10.9767/bcrec.17.4.15923.743-754

1. Introduction

Most building blocks of biomass-derived compounds are in the forms of oxygenates which have a number C–O bonds and higher oxygen content, including sugar alcohols, functionalized carboxylic acids, aldehydes and ketones, phenolic compounds, and furanic derivatives [1–3]. In this sense, the transformation of the oxygenates into high value-added chemicals and fuels using simple supported metal catalysts are quite difficult to catalyze the complexes of C–O bonds. Bimetallic or bifunctional catalyst systems, typically consisted of active metals, supports, and promoters, would be a promising catalyst for feedstocks upgrading. The interaction between metals in the bimetallic or bifunctional catalyst system can modify the properties of catalyst, enhance the activity and selectivity, significantly improve the catalyst stability in presence of biomass-derived impurities or in severe reaction

* Corresponding Author.
Email: rodiansono@ulm.ac.id (R. Rodiansono);
Telp/Fax.: +62-511-4773112

conditions [4,5]. Bimetallic platinum-group metals (PGM) are the most studied catalyst components in the forms of bimetallic or alloy structures owing to it offers many possibilities [6–10]. However, the utilization of PGM-based catalysts is not economic and less viability in the upgrading of biomass-derived platform industry [11].

Intermetallic structures of Ni-based both bulk and supported have received increasing attention as highly selective heterogeneous catalysts for the hydrogenation of unsaturated carbonyl compounds or the transformation of biomass-derived compounds to produce fuels and chemical platforms [12,13]. For example, Shimazu groups developed both bulk and supported bimetallic Ni–M (M = Sn, In, Fe) catalysts for the selective hydrogenation of various a,b-unsaturated carbonyl compounds with high activity and selectivity towards to unsaturated alcohols [14–21]. The dispersion of Ni_3Sn_2 alloy species on metal oxide supports such as TiO_2 to form Ni_3Sn_2/TiO_2 significantly enhanced the activity and chemoselectivity towards hydrogenation of nitro compounds to unsaturated amines [22,23].

In literatures, several synthetic methods of intermetallic Ni-Sn catalyst have been developed (*e.g.,* polyol method, coprecipitation-hydrothermal, surface organometallic chemistry on metal (SOMC/M), chemical vapor deposition (CVD), layered double hydroxide (LDH) route, and arc melting). To obtain bimetallic Ni-Sn alloy catalysts, the utilization of chloride or nitrate metal salts precursors are common approaches, although metal complexes or organometallic salts were also employed. Onda *et al*. prepared Ni-Sn intermetallic from Ni and Sn powder using *arc* melting method under argon atmosphere at above melting point of Ni (1733 K) for 13 h [24]. Komatsu *et al*. [25] and Dumesic *et al.* [26,27] employed organotin ($Sn(CH_3)_4$) and Ni/SiO_2 for the synthesis of $Ni-Sn/SiO_2$ catalysts using CVD method. Marakatti *et al*. reported the synthesis of bulk Ni_3Sn_2 alloy catalysts from LDH route by annealing at 1073 K for 24 h under hydrogen atmosphere [28]. Arc melting, CVD method, and LDH routes seem to be energy consumption, required expensive precursors, and difficult to control the end of Ni–Sn alloy results. Therefore, the development of synthetic protocol that lower energy consumption, utilize inexpensive precursors, and relatively easily handling during the synthesis and catalytic reaction is still challenging.

In the present report, an extended investigation of the effect of temperature annealing on the formation of Ni_3Sn_2 alloy synthesized from different two types of nickel precursors are described. The composition of Ni to Sn was precisely amounted to obtain Ni/Sn molar ratio of 1.4-1.5 from two types nickel precursors: *first*, from Raney nickel supported on aluminium hydroxide (Raney®-Ni/AlOH), which produced as-prepared nickel-tin alloy supported on aluminium hydroxide (Ni-Sn(1.4)/AlOH) [14] and, *second*, from nickel salts (*e.g.,* $NiCl_2$ or $NiCl_2.6H_2O$ or $Ni(acetate)_2$) and produced both bulk and supported Ni-Sn (1.5) alloys [15]. The applied temperatures for the synthesis Ni-Sn alloy were around 573-873 K under H_2 stream for 1.5 h then followed by XRD, N_2 adsorption (BET method), H_2-chemisorption, and NH_3-TPD analyses. The synthesized Ni_3Sn_2 alloy catalysts were tested in selective hydrogenation of biomass-derived furfural to furfuryl alcohol.

2. Materials and Methods

2.1 Materials

Raney Ni-Al alloy ((50%wt of Ni and 50%wt of Al) was purchased from Kanto Chemical Co. Inc.) and used as received. Nickel (II) chloride hexahydrate ($NiCl_2.6H_2O$) and tin (II) chloride dihydrate ($SnCl_2.2H_2O$), and NaOH pellet were purchased from Wako Pure Chemical Co. Ltd. and used as received unless stated otherwise. Furfural (FFald) (98% GC), furfuryl alcohol (FFalc) (98% GC), tetrahydrofurfuryl alcohol (THFalc) (98% GC), *iso*-propanol (*iso*-PrOH; 99.5% GC) were purchased from Tokyo Chemical Industry Co. Ltd. and all organic chemical compounds were purified using standard procedures prior to use. γ–Al_2O_3 (S_{BET} = 100 $m^2.g^{-1}$) were purchased from Japan Aerosil Co.

2.2 Catalyst Preparation

2.2.1 Bulk and Supported Ni_3Sn_2

A typical procedure of the synthesis of bulk Ni_3Sn_2 alloy catalyst is described as follows [15]. $NiCl_2.6H_2O$ (7.2 mmol) was dissolved in deionized water (denoted as solution A), and $SnCl_2.2H_2O$ (4.8 mmol) was dissolved in ethanol/2-methoxy ethanol (2:1) (denoted as solution B) at room temperature. Solutions A and B were mixed at room temperature; the temperature was subsequently raised to 323 K and the mixture was stirred for 12 h. The pH of the mixture was adjusted to 12 through the dropwise addition of an aqueous solution of 3.1 M NaOH. The mixture was then placed into a sealed-Teflon autoclave for the hydrothermal reaction at 423 K for 24 h. The resulting black

precipitate was filtered, washed with distilled water, and then dried under vacuum overnight. Prior to the catalytic reaction, the obtained black powder was treated under hydrogen at 673 K for 90 min. The procedure of the synthesis of γ-Al_2O_3 supported Ni_3Sn_2 (Ni_3Sn_2/γ-Al_2O_3) was similar to the bulk, whereas a 1.0 g γ-Al_2O_3 (S_{BET} = 100 $m^2.g^{-1}$) was added to solution mixture before the hydrothermal at 423 K for 24 h. The obtained Ni_3Sn_2/γ-Al_2O_3 then was reduced with H_2 gas at 573, 673, 773, 873 K for 1.5 h and Ni_3Sn_2/γ-Al_2O_3 was obtained.

2.2.2 Synthesis of Supported Ni-Sn(1.4)/AA

Typical procedure of the supported Ni-Sn(1.4)/AA; 1.4 = Ni/Sn molar ratio and AA = amorphous alumina) catalysts is described as the follows [20]. Raney®Ni/AlOH (it was obtained from alkali leaching of Raney Ni-Al alloy according to Petro`s protocol [29]) was mixed with a solution that contained 0.45 mmol $SnCl_2.2H_2O$ at room temperature and stirred for 2 h. The mixture was placed into a sealed-Teflon autoclave reactor for the hydrothermal treatment at 423 K for 2 h. The resulting precipitate was filtered, washed with distilled water and ethanol, and dried under vacuum overnight then the as-prepared Ni-Sn(1.4)/AlOH was produced. The as-prepared Ni-Sn(1.4)/AlOH sample then was reduced with H_2 gas at 573, 673, 773, 873 K for 1.5 h and Ni-Sn(1.4)/AA; AA = amorphous alumina was obtained [30,31].

2.3 Catalyst Characterization

The bulk compositions of the catalysts were determined by inductively coupled plasma-atomic emission spectroscopy (ICP-AES), using an SPS1700 HVR of SII instrument. Powder X-ray diffraction was taken on a Mac Science M18XHF instrument using monochromatic CuKα radiation (λ = 0.15418 nm). It was operated at 40 kV and 200 mA with a step width of 0.02° and a scan speed of 4° min^{-1}. The formation of Ni-Sn alloy for every sample was confirmed by ICDD standard data [32]. The mean crystallite size of Ni-Sn was calculated from the full width at half maximum (FWHM) of the Ni_3Sn_2(110) alloy diffraction peak according to the Scherrer equation.

The BET surface area (S_{BET}) and pore volume (V_p) were measured using N_2 physisorption at 77 K on a Belsorp Max (BEL Japan). The samples were degassed at 473 K for 2 h to remove physisorbed gases prior to the measurements. The amount of nitrogen adsorbed onto the samples was used to calculate the BET surface area via the BET equation. The pore volume was estimated to be the liquid volume of nitrogen at a relative pressure of approximately 0.995 according to the Barrett–Joyner–Halenda (BJH) approach based on desorption data.

The H_2 uptake was determined by H_2 chemisorption. After the catalyst was heated at 393 K under vacuum for 30 min, it was heated at 673 K under H_2 for 30 min and under vacuum for 30 min, followed by evacuation to room temperature for 30 min. The adsorption of H_2 was conducted at 273 K.

2.4 Catalytic Reactions

2.4.1 General Procedure for Hydrogenation of FFald

Catalyst (0.05 g), FFald (1.1 mmol), and *iso*-propanol (*iso*-PrOH) (3 mL) as solvent were placed into a glass reaction tube, which fit inside a stainless-steel reactor. After H_2 was introduced into the reactor with an initial H_2 pressure of 3.0 MPa at room temperature, the temperature of the reactor was increased to 453 K. After 75 min, the conversion of FFald and the yield of FFalc were determined via GC analysis. The Ni-Sn(1.4)/AA 673$H_{2red.}$ catalyst was easily separated using either simple centrifugation or filtration.

2.4.2 Product Analysis

Gas chromatography (GC) analysis of the reactant (FFald) and products (FFalc, THFalc) was performed on a Perkin Elmer Autosystem XL with a flame ionization detector with an InertCap 225 (i.d. 0.25 mm, length 30 m, d.f. 0.25 mm) capillary column of GL Science Inc. Tokyo Japan. Gas chromatography-mass spectrometry (GC-MS) was performed on a Shimadzu GC-17B equipped with a thermal conductivity detector and an RT-βDEXsm capillary column. The products were confirmed by a comparison of their GC retention time, mass spectra with those of authentic samples.

The conversion, yield and selectivity of the products were calculated according to the following equations:

$$Conversion = \frac{F_0 - F_t}{F_0} \times 100\% \quad (1)$$

$$Yield = \frac{mol\ product}{consumed\ mol\ reactant} \times 100\% \quad (2)$$

$$Selectivity = \frac{mol\ product}{total\ mol\ products} \times 100\% \quad (3)$$

where F_0 is the introduced mol reactant (furfural, FFald), F_t is the remaining mol reactant, and ΔF is the consumed mol reactant (introduced mol reactant- remained mol reactant), which are all obtained from GC analysis using an internal standard technique.

3. Results and Discussion

3.1 Catalyst Characterization

The physicochemical properties of bulk and supported Ni_3Sn_2/γ–Al_2O_3, and Ni-Sn(1.4)/AA catalysts are summarized in Table 1. It can be observed that S_{BET} of bulk Ni_3Sn_2 was only 12 $m^2.g^{-1}$, while supported Ni_3Sn_2/AA and Ni-Sn(1.4)/AA were 95 $m^2.g^{-1}$ and 27 $m^2.g^{-1}$, respectively. The H_2 uptake of supported Ni_3Sn_2/γ-Al_2O_3 and Ni-Sn(1.4)/AA was 37 $\mu mol.g^{-1}$ and 32 $\mu mol.g^{-1}$, respectively which is higher than that the bulk (8.6 $\mu mol.g^{-1}$). These results suggest that higher dispersion of Ni_3Sn_2 alloy particles on AA were formed as roughly depicted in the average Ni_3Sn_2(101) crystallite sizes, which were 14.7 nm and 15 nm, respectively (entries 2 and 3). These results are also comparable to the previous results of Marakatti [28], Komatsu [33], Agnelli [34].

To identify the formation of Ni-Sn alloy phases in each sample, the XRD patterns of each sample and crystallographic data were compared with JCPDS card number of #35-1362 for Ni_3Sn, #06-414 for Ni_3Sn_2, #04-0850 for nickel metal, and #06-395 for tin metal/tin oxide. The XRD patterns of bulk Ni_3Sn_2, Ni_3Sn_2/γ-Al_2O_3 as prepared, and Ni-Sn(1.4)/AA as prepared and after reduction with H_2 treatment at 573-873 K are shown in Figure 1, Figure 2, and Figure 3, respectively. Multi-

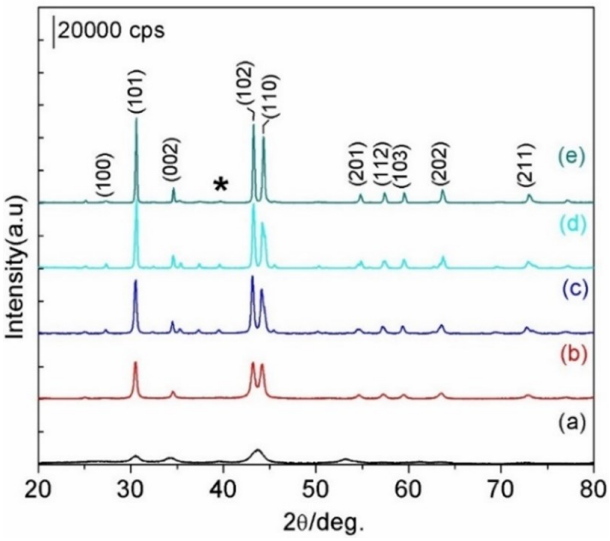

Figure 1. XRD patterns of bulk Ni_3Sn_2 (a) *as prepared* and after reduction with H_2 at temperature of (b) 573 K, (c) 673 K, (d) 773 K, and (e) 873 K for 1.5 h. The plotted data were compared with JCPDS card of #06-414. (*) Ni_3Sn.

Table 1. Physico-chemical properties of bulk Ni_3Sn_2, supported Ni_3Sn_2/AA, and Ni-Sn(1.4)/AA catalysts after reduction with H_2 at 573-873 K for 1.5 h.

Entry	Catalyst[a]	Composition[b] (mol%) and [major alloy phase][c]	S_{BET}[c] ($m^2.g^{-1}$)	H_2 uptake[d] ($\mu mol.g^{-1}$)	Crystallite sizes[e] (nm)
1	Bulk Ni_3Sn_2 *as prepared*	$Ni_{59.9}Sn_{40.1}$	70.3	nd	na
2	Bulk Ni_3Sn_2 573$H_{2red.}$	$Ni_{59.9}Sn_{40.1}$ [Ni_3Sn_2]	9.7	nd	15.1
3	Bulk Ni_3Sn_2 673$H_{2red.}$	$Ni_{59.9}Sn_{40.1}$ [Ni_3Sn_2 91%]	12	8.6	17.0
4	Bulk Ni_3Sn_2 773$H_{2red.}$	$Ni_{59.9}Sn_{40.1}$ [Ni_3Sn_2]	2.1	6.1	26.5
5	Bulk Ni_3Sn_2 873$H_{2red.}$	$Ni_{59.9}Sn_{40.1}$ [Ni_3Sn_2]	3.2	4.7	34.2
6	Ni_3Sn_2/γ-Al_2O_3 *as prepared*	$Ni_{60.0}Sn_{40.0}$	115	nd	8.9
7	Ni_3Sn_2/γ-Al_2O_3 573$H_{2red.}$	$Ni_{60.0}Sn_{40.0}$	79	nd	9.7
8	Ni_3Sn_2/γ-Al_2O_3 673$H_{2red.}$	$Ni_{60.0}Sn_{40.0}$ [Ni_3Sn_2 90%]	120	37	11.4
9	Ni_3Sn_2/γ-Al_2O_3 773$H_{2red.}$	$Ni_{60.0}Sn_{40.0}$ [Ni_3Sn_2]	79	27	13.7
10	Ni_3Sn_2/γ-Al_2O_3 873$H_{2red.}$	$Ni_{60.0}Sn_{40.0}$ [Ni_3Sn_2]	76	9.1	22.8
11	Ni-Sn(1.4)/AlOH *as prepared*	$Ni_{34.9}Sn_{24.8}Al_{40.4}$	82	75	na
12	Ni-Sn(1.4)/AA 573$H_{2red.}$	$Ni_{34.9}Sn_{24.8}Al_{40.4}$	nd	nd	5.2
13	Ni-Sn(1.4)/AA 673$H_{2red.}$	$Ni_{34.9}Sn_{24.8}Al_{40.4}$ [Ni_3Sn_2 88%]	50	60	14.7
14	Ni-Sn(1.4)/AA 773$H_{2red.}$	$Ni_{34.9}Sn_{24.8}Al_{40.4}$ [Ni_3Sn_2 85%]	26	40	16.6
15	Ni-Sn(1.4)/AA 873$H_{2red.}$	$Ni_{34.9}Sn_{24.8}Al_{40.4}$ [Ni_3Sn_2]	27	36	28.4

[a]Value in the parenthesis is Ni/Sn molar ratio. [b]The composition was determined by using ICP-AES. [c]Based on the crystallographic databases [32] and mol% of alloy component was calculated by Multi-Rietveld Analysis Program LH-Riet 7.00 method on the Rietica software. [c]Determined by N_2 adsorption at 77 K. [d]Based on the total H_2 uptake at 273 K (noted after corrected for physical and chemical adsorption). [e]Caclulated by using Scherrer`s equation on Ni_3Sn_2(101). nd = not determined. na = not available.

Rietveld Analysis Program LH-Riet on the Rietica software was performed to the powder X-ray diffraction patterns of bulk Ni_3Sn_2 $673H_{2red}$, $Ni_3Sn_2/\gamma\text{-}Al_2O_3$ $673H_{2red}$, Ni-Sn(1.4)/AA $673H_{2red}$, and Ni-Sn(1.4)/AA $773H_{2red}$ and it was found that the amount of Ni_3Sn_2 alloy species was 91% (entry 3), 90% (entry 8), 88% (entry 13), and 85% (entry 14), respectively.

In the case of the as prepared bulk Ni_3Sn_2 alloy (Figure 1), the broadened peaks at 2θ of 30.5°, 34.4°, and 43.7° which are recognized as Ni_3Sn_2(101), Ni_3Sn_2(002), Ni_3Sn_2(102), Ni_3Sn_2(110) alloy phases were observed (Figure 1(a)). After reduction with H_2 at 573, 673, 773, and 873 K, the diffraction peaks become intensified and a series Ni_3Sn_2 alloy phase system were formed with almost single phase. A small peak at 2θ of 39.3° was also observed which can be assigned as Ni_3Sn(200) alloy phase [32]. These results suggest that the crystallite sizes of Ni_3Sn_2 alloy particle become higher, as roughly depicted from crystallite sizes of Ni_3Sn_2(101) which were 15.1 nm, 17.0 nm, 26.5 nm, and 34.2 nm, respectively (Table 1, entries 2-5). The specific surface area (S_{BET}) and H_2 uptakes are also consistent with the average crystallite sizes of Ni_3Sn_2 alloy, whereas both S_{BET} and H_2 uptakes decreased significantly after reduction with H_2 at 673-873 K.

For supported $Ni_3Sn_2/\gamma\text{-}Al_2O_3$ samples, similar XRD profiles are also obtained for both the as prepared and after reduction with H_2 at 573-873 K (Figure 2). For example, the crystal growth of Ni_3Sn_2(102) and Ni_3Sn_2(110) was easily observed as function of temperature as well as Ni_3Sn_2(101). The average crystallite sizes of Ni_3Sn_2(101) were 8.9 nm (for the as prepared) and increased to 9.7 nm, 11.4 nm, 13.7 nm, and 22.8 nm after reduction with H_2 at 573, 673, 773, and 873 K, respectively. The S_{BET} and H_2 uptakes also suggest that the controlled annealing under H_2 atmosphere may mainly affect to the physico-chemical properties of supported $Ni_3Sn_2/\gamma\text{-}Al_2O_3$ as summarized in Table 1 (entries 6-10).

In the case of Ni-Sn(1.4)/AA catalyst (Figure 3), the Ni/Sn molar ratio of 1.4 was found to be the best composition and demonstrated a highly active and selective in the hydrogenation of biomass-derived furfural and levulinic acid have been reported previously [14,20,30]. It can be observed that broadened peaks with hardly to distinguish due to the overlapping of diffraction peaks of Ni or bimetallic Ni-Sn alloy were formed on the as prepared and H_2 treated at 573 K. After H_2 treatment at 673-773 K for 1.5 h, a series Ni_3Sn_2 alloy phases were clearly observed, and a broadened peak at 2θ of 44.6° was split up into two peaks which were easily recognized as Ni_3Sn_2(102) and Ni_3Sn_2(110) alloy phases (Figure 3(c)-(d)). Further treatment at higher temperature of 873 K, all diffraction peaks intensified and small peaks at 2θ of 39.3° and 43.0° which are assigned as Ni_3Sn(200) and Ni_3Sn(002) alloy phases, respectively, were also observed [32] (Figure 3(e)).

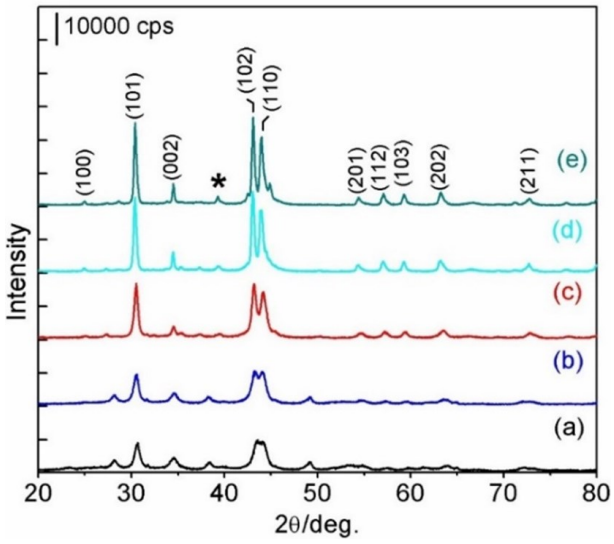

Figure 2. XRD patterns of supported $Ni_3Sn_2/\gamma\text{-}Al_2O_3$ (a) *as prepared* and after reduction with H2 at temperature of (b) 573 K (c) 673 K, (d) 773 K, and (e) 873 K. The plotted data were compared with JCPDS card of #06-414. (*) Ni_3Sn.

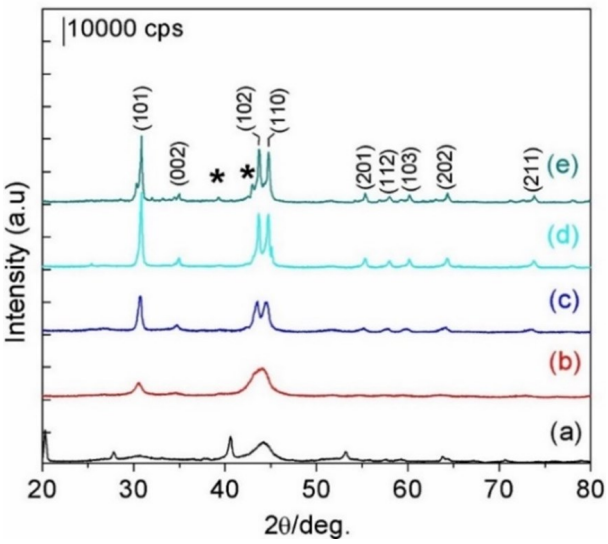

Figure 3. XRD patterns of supported Ni-Sn(1.4)/AA (a) *as prepared*, and after reduction with H_2 at temperature of (b) 573 K, (c) 673 K, (d) 773 K, and (e) 873 K for 1.5 h. The plotted data were compared with JCPDS card of #06-414. (*) Ni_3Sn.

The S_{BET} and H_2 uptakes decreased to almost in half after reduction with H_2 at 673-873 K while the average crystallite sizes of Ni_3Sn_2(101) increased gradually as the increase of temperature (Table 1, entries 11-15). On the other hand, the diffraction peaks of bayerite and gibbsite completely disappeared after H_2 treatment at 673 K, indicating the transformation of crystalline bayerite or gibbsite into amorphous alumina which have no detectable peaks in XRD analysis [35–37]. Additionally, the diffraction peak of metallic Ni(200) and Ni(220) species disappeared completely in the as-prepared and observed after H_2 treatment, suggesting the formation of Ni-Sn alloy might be selectively occurred on the surface of Ni(111) rather than on the surface of Ni(200) or Ni(220) [38–40].

The amount of acid sites (μmol.g^{-1}) of each synthesized bulk Ni_3Sn_2 673H_{2red}. and supported alloy catalysts was measured by using ammonia (NH_3) as molecular probe as shown in Figure 4 and the results are also summarized in Table 2. Bulk Ni_3Sn_2 673H_{2red} has amount of acid sites of 133 μmol.g^{-1}, while amount of acid sites of Ni_3Sn_2/γ-Al_2O_3 673H_{2red} was 276 μmol.g^{-1} which is almost two times higher than that of the bulk catalyst. Ni-Sn(1.4)/AA 673H_{2red} has a maximum acid density (346 μmol.g^{-1}) and the acid density drastically dropped to 117 μmol.g^{-1} after reduction with H_2 at 873 K (entry 4). It can be suggested that the acid density of supported Ni_3Sn_2 is likely due to the great contribution of aluminium oxide or aluminium hydroxide of support (Figures 4(a)-(d)) or which also depend on the atomic arrangement in bimetallic Ni-Sn alloy crystal forms [15,28,38]. The total acidity of each catalyst is estimated from the desorbed amount of NH_3 without further identification of acid types, because it is difficult to distinguish the weak, medium and strong acid sites from such broad desorption peaks. The quantification results are summarized in Table 2.

Table 2. Results of total NH_3 acidity bulk and supported Ni_3Sn_2 after reduction with H_2 at 673 K for 1.5 h.

Entry	Catalyst[a]	Amount of acid sites[b] (μmol.g^{-1})
1	Ni_3Sn_2 673$H_{2red.}$	133
2	Ni_3Sn_2/γ-Al_2O_3 673$H_{2red.}$	276
3	Ni-Sn(1.4)/AA 673$H_{2red.}$	346
4	Ni-Sn(1.4)/AA 873$H_{2red.}$	117

[a]The value in the parenthesis is Ni/Sn ratio, determined by ICP-AES. [b]Amount of acid sites (μmol g^{-1}) was derived from NH_3-TPD spectra.

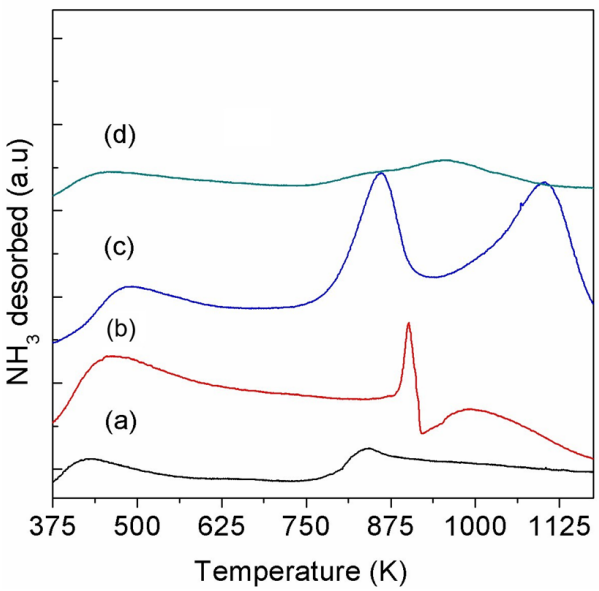

Figure 4. NH_3-TPD of (a) bulk Ni_3Sn_2 673$H_{2red.}$, (b) Ni_3Sn_2/γ-Al_2O_3 673$H_{2red.}$, (c) Ni-Sn(1.4)/AA 673$H_{2red.}$, and (d) Ni-Sn(1.4)/AA 873H_{2red}.

Table 3. Results of FFald hydrogenation over the bulk and supported Ni_3Sn_2 catalysts after H_2 treatment at 673 K for 1.5 h.

Entry	Catalyst[a]	Conversion (%)	Yield[b] (%)	Selectivity (%)	
				FFalc	THFalc
1	Bulk Ni_3Sn_2 *as prepared*	49.8	27.4	86	14
2	Bulk Ni_3Sn_2 573$H_{2red.}$	96	57.5	82	18
3	Ni_3Sn_2/γ-Al_2O_3 *as prepared*	56.4	56.3	100	0
4	Ni_3Sn_2/γ-Al_2O_3 573$H_{2red.}$	100	99.1	99	1
5	Ni-Sn(1.4)/AlOH *as prepared*	98	91	94	6
6	Ni-Sn(1.4)/AA 573$H_{2red.}$	100	98	98	2

[a]The value in the parenthesis is Ni/Sn molar ratio. Reaction conditions: FFald, 0.04 g (FFald/Ni ratio = ~15); iso-PrOH (3 mL); H_2, 3.0 MPa, 453 K, 75 min. [b]Yield of FFalc, determined by GC using an internal standard technique.

3.2 Catalytic Reactions

3.2.1 Furfural hydrogenation

Results for the selective hydrogenation of FFald using bulk and supported Ni_3Sn_2 alloy catalysts are summarized in Table 3, and the reaction pathways are shown in Scheme 1. Over the *as prepared* bulk Ni_3Sn_2 alloy catalyst, FFald conversion was 49.8% with a furfuryl alcohol (FFalc) yield of 27.4% or the selectivity to FFalc and tetrahydrofurfuryl alcohol (THFalc) were 86.2% and 13.8%, respectively (Table 3, entry 1). After reduction with H_2 at 573 K, the conversion of FFald increased two times (96%) with FFalc and THFalc selectivities of 82% and 18%, respectively (entry 2) under the same reaction conditions.

Figure 5 shows the effect of temperature H_2 reduction over bulk Ni_3Sn_2 alloy catalyst at the temperature range of 573-873 K for 1.5 h. It can be observed that high FFald conversion was achieved over bulk Ni_3Sn_2 573$H_{2red.}$ and Ni_3Sn_2 673$H_{2red.}$ catalysts with also high selectivity to FFalc. In contrast, bulk Ni_3Sn_2 reduced at 773 K (Ni_3Sn_2 773H_{2red}) gave only 10% FFald conversion with FFalc and THFalc selectivities were 65% and 35% and further reduction at higher temperature (873 K) dropped the FFald conversion (only 6%) as well as FFalc selectivity. These results suggest that controlled-annealing temperature in the preparation and activation of bulk Ni_3Sn_2 alloy catalyst is substantially required to obtain high activity and selectivity. Therefore, it can be concluded that the optimized temperature for the preparation bulk Ni_3Sn_2 alloy catalyst was 673 K.

For the *as prepared* Ni_3Sn_2/γ-Al_2O_3 catalyst, FFald conversion was 56.4% with a FFalc yield of 56.3% (almost 100% selectivity, Table 3, entry 3), whereas the as prepared Ni-Sn(1.4)/AlOH catalyst produced FFalc yield of 91% (entry 4). A remarkably high FFald conversion (>99) and FFalc selectivity (98-99%) were obtained when Ni_3Sn_2/γ-Al_2O_3 573$H_{2red.}$ and Ni-Sn(1.4)/AA 573$H_{2red.}$ were used under the same reaction conditions (Table 3, entries 4 and 6). The high conversion of FFald and the high selectivity of FFalc over Ni_3Sn_2/γ-Al_2O_3 573$H_{2red.}$ and Ni-Sn(1.4)/AA 573$H_{2red.}$ may be attributed to the relatively high dispersion of Ni-Sn alloy on amorphous alumina giving rise to active sites with a significantly higher catalytic activity. Further H_2 reduction both the *as*

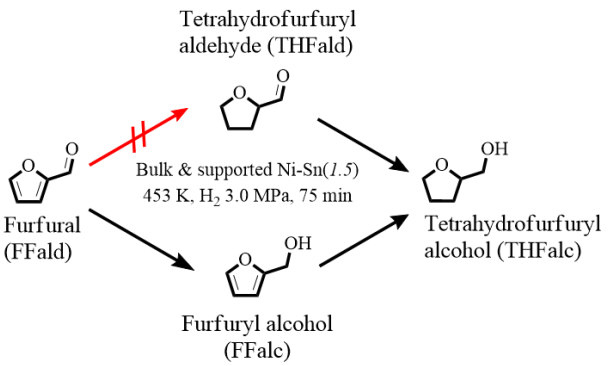

Scheme 1. Reaction pathways of FFald hydrogenation over the bulk and supported Ni_3Sn_2 alloy catalysts.

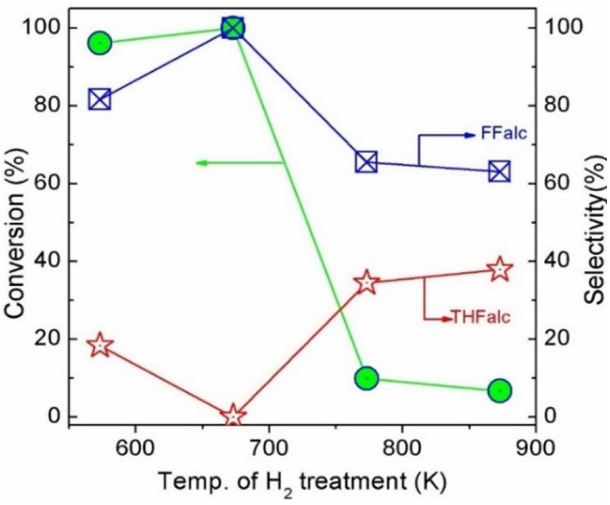

Figure 5. Effect of temperature reduction with H_2 on the conversion and selectivity in the selective hydrogenation of furfural for bulk Ni_3Sn_2 alloy catalysts. *Reaction conditions*: FFald, 0.04 g (FFald/Ni ratio = ~15); *iso*-PrOH (3 mL); H_2, 3.0 MPa, 453 K, 75 min.

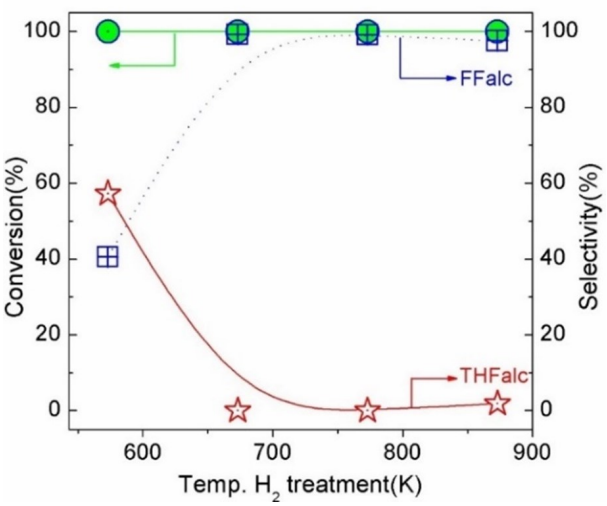

Figure 6. Effect of temperature reduction with H_2 on the conversion and selectivity in the selective hydrogenation of furfural for supported Ni_3Sn_2/γ-Al_2O_3 alloy catalysts. *Reaction conditions*: FFald, 0.04 g (FFald/Ni ratio = ~15); *iso*-PrOH (3 mL); H_2, 3.0 MPa, 453 K, 75 min.

prepared Ni_3Sn_2/γ-Al_2O_3 and Ni-Sn(1.4)/AlOH at higher temperature c.a. 673-873 K resulted higher crystallinity of Ni_3Sn_2 alloy phase as indicated by XRD patterns (Figures 2 and 3). Interestingly, both Ni_3Sn_2/AA and Ni-Sn(1.4)/AA catalysts gave high FFald conversion and FFalc yield as the increase of temperature H_2 reduction up to 873 K (Figures 6 and 7). These results suggest that genuine structure of Ni_3Sn_2 alloy phase may have played prominent role in the selective hydrogenation of C=O rather than C=C bonds of furfural. Resasco *et al*. have reported that the selective hydrogenation of C=O versus C=C in a,b-unsaturated aldehydes by Pd-Cu alloy supported on silica was caused by the preferential h^2-coordination of C=O to Pd [41–43]. The similar results also were reported recently upon bimetallic Pt-Sn catalyst system that the most preferred configuration of is tilted with the O in C=O group sitting on top of the Sn site then facilitated effectively to high selectivity toward FFalc [44].

3.2.2 Reusability Test

A reusability tests were performed on the Ni_3Sn_2/γ-Al_2O_3 $673H_{2red.}$ and Ni-Sn(1.4)/AA $673H_{2red.}$ catalysts and the results are shown in Figure 8. The used Ni_3Sn_2/γ-Al_2O_3 $673H_{2red.}$ and Ni-Sn(1.4)/AA $673H_{2red.}$ catalysts were easily separated by either simple centrifugation or filtration after the reaction. The spent catalysts were reuse directly without further treatment.

The activity and selectivity of Ni_3Sn_2/γ-Al_2O_3 $673H_{2red.}$ catalyst slightly decreased after the fifth consecutive run in FFald hydrogenation. The amount of Ni and Sn that leached into the reaction solution for FFald hydrogenation was 1.8 mol% and 2.3 mol%, respectively after the fifth run. In contrast, the activity and selectivity of Ni-Sn(1.4)/AA $673H_{2red.}$ maintained for at least five consecutive runs with FFald conversion of >95% and FFalc selectivity of >99%. The amount of metals leaching into the reaction solution in FFald hydrogenation were 0.78 mol% (Ni) and 1.5 mol% (Sn) after the fifth run.

The stability of supported Ni_3Sn_2/γ-Al_2O_3 $673H_{2red}$ catalyst slightly less than that of Ni-Sn(1.4)/AA $673H_{2red.}$ catalyst which were synthesized from different nickel precursors. Consequently, the later catalyst consists of the mixture of Ni-Sn alloy phase (*e.g.*, Ni_3Sn_2) and Ni(0) that may play prominent role in FFald hydrogenation conditions [14,45]. Dumesic [26], Komatsu [46,47], and Linic [40] have shown that carbon tolerance of Ni-based catalysts could be improved by synthesizing Ni-containing surface alloys with the second electropositive metal of tin (Sn). XRD and Mössbauer spectroscopy studies suggested that Sn migrates into the Ni particles to form intermetallic Ni-Sn [48,49], metallic Sn will deposit and diffuse on Ni particles at temperature 448-498 K during chemical vapor deposition (CVD) processes. Results of DFT studies also confirmed that during the formation of Sn/Ni surface alloy, there is a favorable thermodynamic driving force for Sn to displace Ni atom from

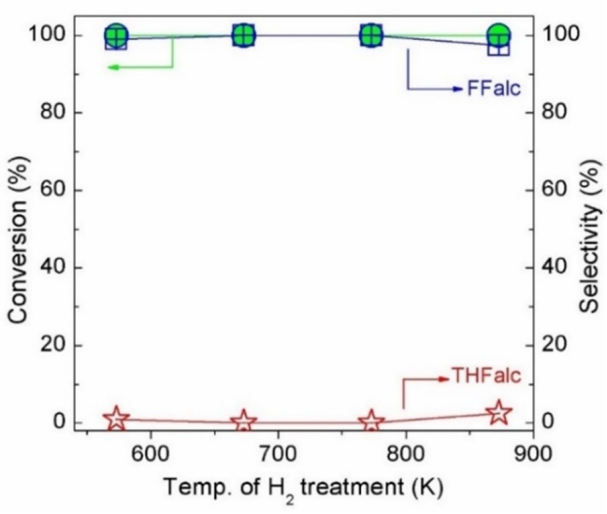

Figure 7. Effect of temperature reduction with H_2 on the conversion and selectivity in the selective hydrogenation of furfural for supported Ni-Sn(1.4)/AA alloy catalysts. *Reaction conditions*: FFald, 0.04 g (FFald/Ni ratio = ~15); *iso*-PrOH (3 mL); H_2, 3.0 MPa, 453 K, 75 min.

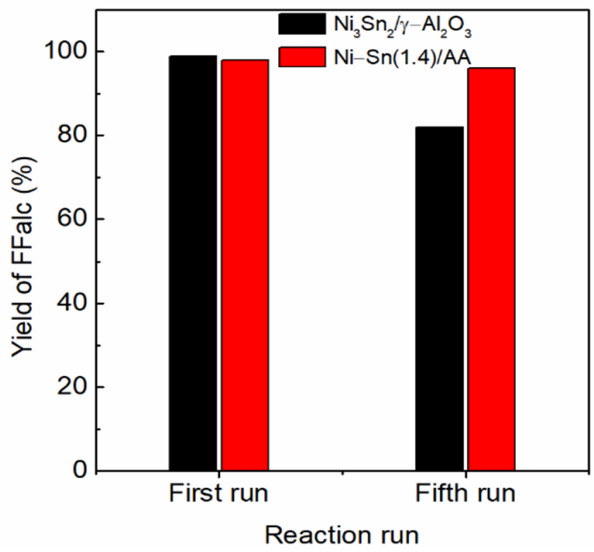

Figure 8. Reusability test of Ni_3Sn_2/γ-Al_2O_3 $673H_{2red.}$ and Ni-Sn(1.4)/AA $673H_{2red.}$ catalysts in FFald hydrogenation. *Reaction conditions*: FFald, 0.04 g (FFald/Ni ratio = ~15); *iso*-PrOH (3 mL); H_2, 3.0 MPa, 453 K, 75 min.

the step-edge sites which effectively repel C atoms from the low-coordinated step sites. Since low-coordinated step sites have been proposed to play a role in the nucleation and growth of carbon deposits over Ni [39], this arrangement of Sn atoms further lowers the tendency of the alloy to form carbon deposits [48].

4. Conclusions

We described the controlled annealing of both bulk and supported Ni_3Sn_2 alloy catalysts under hydrogen atmosphere at elevated temperature of 573-873 K for 1.5 h. After reduction with H_2 at 573, 673, 773, and 873 K, the diffraction peaks of a series Ni_3Sn_2 alloy phase systems were formed with almost single phase. The crystallite sizes of Ni_3Sn_2 alloy particle become higher, as roughly depicted from crystallite sizes of Ni_3Sn_2(101). The specific surface area (S_{BET}) and H_2 uptakes decreased significantly after reduction with H_2 at 673-873 K for both bulk and supported Ni_3Sn_2 alloy. The controlled-annealing temperature in the preparation and activation of bulk and supported Ni_3Sn_2 alloy catalyst is substantially required to obtain high activity and selectivity. The optimized temperature for the preparation bulk Ni_3Sn_2 alloy, Ni_3Sn_2/γ-Al_2O_3, and Ni-Sn(1.4)/AA catalysts was 673 K and 573-773 K, respectively and produced almost single phase Ni_3Sn_2 with the best catalytic performance for the selective hydrogenation of furfural to furfuryl alcohol. The activity and selectivity of Ni-Sn(1.4)/AA $673H_{2red.}$ maintained for at least five consecutive runs both in FFald hydrogenation with FFald conversion of >95% and FFalc selectivity of >99% which is relatively higher stability than that of Ni_3Sn_2/γ-Al_2O_3 $673H_{2red}$.

Acknowledgements

This work was financially supported by Hibah Penelitian Dasar Kompetitif Nasional (PDKN) FY 2021-2023 under grant number of 026/E5/PG.02.00.PT/2022 from Ministry of Education, Culture, Research & Technology, Republic of Indonesia.

CrediT Author Statement

Rodiansono: Conceptualization, Methodology, Investigation, Writing-Original draft, Writing-Review & Editing. **Atina Sabila Azzahra:** Formal Analysis, Investigation. **Sadang Husain** and **Pathur Razi Ansyah**: Visualization.

References

[1] Bozell, J.J., Petersen, G.R. (2010). Technology development for the production of biobased products from biorefinery carbohydrates—the US Department of Energy's "top 10" revisited. *Green Chemistry*, 12(4), 539–55. DOI: 10.1039/b922014c.

[2] Clark, J.H., Luque, R., Matharu, A.S. (2012). Green Chemistry, Biofuels, and Biorefinery. *Annual Review of Chemical and Biomolecular Engineering*, 3(1), 183–207. DOI: 10.1146/annurev-chembioeng-062011-081014.

[3] Esposito, D., Antonietti, M. (2015). Redefining biorefinery: the search for unconventional building blocks for materials. *Chemical Society Reviews*, 44(16), 5821–5835. DOI: 10.1039/c4cs00368c.

[4] Alonso, D.M., Wettstein, S.G., Dumesic, J.A. (2012). Bimetallic catalysts for upgrading of biomass to fuels and chemicals. *Chemical Society Reviews*, 41(24), 8075–8098. DOI: 10.1039/c2cs35188a.

[5] Tomishige, K., Nakagawa, Y., Tamura, M. (2020). Design of supported metal catalysts modified with metal oxides for hydrodeoxygenation of biomass-related molecules. *Current Opinion in Green and Sustainable Chemistry*, 22, 13–21. DOI: 10.1016/j.cogsc.2019.11.003.

[6] Sachtler, W.M.H., van Santen, R.A. (1977). Surface Composition and Selectivity of Alloy Catalysts. *Advances in Catalysis*, 26(C), 69–119. DOI: 10.1016/S0360-0564(08)60070-X.

[7] Sankar, M., Dimitratos, N., Miedziak, P.J., Wells, P.P., Kiely, C.J., Hutchings, G.J. (2012). Designing bimetallic catalysts for a green and sustainable future. *Chemical Society Reviews*, 41(24), 8099–8139. DOI: 10.1039/c2cs35296f.

[8] Li, X., Wan, W., Kattel, S., Chen, J.G., Wang, T. (2016). Selective hydrogenation of biomass-derived 2(5H)-furanone over Pt-Ni and Pt-Co bimetallic catalysts: From model surfaces to supported catalysts. *Journal of Catalysis*, 344, 148–156. DOI: 10.1016/j.jcat.2016.09.027.

[9] Kon, K., Onodera, W., Takakusagi, S., Shimizu, K.I. (2014). Hydrodeoxygenation of fatty acids and triglycerides by Pt-loaded Nb2O5catalysts. *Catalysis Science and Technology*, 4(10), 3705–3712. DOI: 10.1039/c4cy00757c.

[10] Sun, K.Q., Hong, Y.C., Zhang, G.R., Xu, B.Q. (2011). Synergy between Pt and Au in Pt-on-Au nanostructures for chemoselective hydrogenation catalysis. *ACS Catalysis*, 1(10), 1336–1346. DOI: 10.1021/cs200247r.

[11] Xue, Z., Liu, Q., Wang, J., Mu, T. (2018). Valorization of levulinic acid over non-noble metal catalysts: Challenges and opportunities. *Green Chemistry*, 20(19), 4391–4408. DOI: 10.1039/c8gc02001a.

[12] De, S., Zhang, J., Luque, R., Yan, N. (2016). Ni-based bimetallic heterogeneous catalysts for energy and environmental applications. *Energy and Environmental Science*, 9(11), 3314–3347. DOI: 10.1039/c6ee02002j.

[13] Ghatak, A., Das, M. (2021). The Recent Progress on Supported and Recyclable Nickel Catalysts towards Organic Transformations: A Review. *ChemistrySelect,* 6(15), 3656–3682. DOI: 10.1002/slct.202100727.

[14] Rodiansono, R., Hara, T., Ichikuni, N., Shimazu, S. (2012). A novel preparation method of Ni-Sn alloy catalysts supported on aluminium hydroxide: Application to chemoselective hydrogenation of unsaturated carbonyl compounds. *Chemistry Letters*, 41(8), 769–771. DOI: 10.1246/cl.2012.769.

[15] Rodiansono, R., Khairi, S., Hara, T., Ichikuni, N., Shimazu, S. (2012). Highly efficient and selective hydrogenation of unsaturated carbonyl compounds using Ni-Sn alloy catalysts. *Catalysis Science and Technology*, 2(10), 2139–2145. DOI: 10.1039/c2cy20216f.

[16] Putro, W.S., Hara, T., Ichikuni, N., Shimazu, S. (2017). Efficiently recyclable and easily separable Ni-Fe alloy catalysts for chemoselective hydrogenation of biomass-derived furfural. *Chemistry Letters*, 46(1), 149–151. DOI: 10.1246/cl.160905.

[17] Putro, W.S., Kojima, T., Hara, T., Ichikuni, N., Shimazu, S. (2017). Selective hydrogenation of unsaturated carbonyls by Ni-Fe-based alloy catalysts. *Catalysis Science & Technology*, 7(16), 3637–3646. DOI: 10.1039/c7cy00945c.

[18] Rodiansono, R., Astuti, M.D., Santoso, U.T., Shimazu, S. (2015). Hydrogenation of Biomass-derived Furfural Over Highly Dispersed-Aluminium Hydroxide Supported Ni-Sn(3.0) Alloy Catalysts. *Procedia Chemistry*, 16, 531–539. DOI: 10.1016/j.proche.2015.12.089.

[19] Rodiansono, R., Astuti, M.D., Khairi, S., Shimazu, S. (2016). Selective hydrogenation of biomass-derived furfural over supported Ni3Sn2 alloy: Role of supports. *Bulletin of Chemical Reaction Engineering & Catalysis*, 11(1), 1–9. DOI: 10.9767/bcrec.11.1.393.1-9.

[20] Rodiansono, R., Hara, T., Ichikuni, N., Shimazu, S. (2014). Development of nanoporous Ni-Sn alloy and application for chemoselective hydrogenation of furfural to furfuryl alcohol. *Bulletin of Chemical Reaction Engineering and Catalysis*, 9(1), 53–59. DOI: 10.9767/bcrec.9.1.5529.53-59.

[21] Rodiansono, R., Astuti, M.D., Mujiyanti, D.R., Santoso, U.T., Shimazu, S. (2018). Novel preparation method of bimetallic Ni-In alloy catalysts supported on amorphous alumina for the highly selective hydrogenation of furfural. *Molecular Catalysis*, 445, 52–60. DOI: 10.1016/j.mcat.2017.11.004.

[22] Yamanaka, N., Hara, T., Ichikuni, N., Shimazu, S. (2019). Chemoselective hydrogenation of 4-nitrostyrene to 4-aminostyrene by highly efficient TiO2 supported Ni3Sn2 alloy catalyst. *Bulletin of the Chemical Society of Japan*, 92(4), 811–816. DOI: 10.1246/bcsj.20180381.

[23] Yamanaka, N., Hara, T., Ichikuni, N., Shimazu, S. (2018). Chemoselective hydrogenation of unsaturated nitro compounds to unsaturated amines by Ni-Sn alloy catalysts. *Chemistry Letters*, 47(8), 971–974. DOI: 10.1246/cl.180458.

[24] Onda, A., Komatsu, T., Yashima, T. (2000). Characterization and catalytic properties of Ni-Sn intermetallic compounds in acetylene hydrogenation. *Physical Chemistry Chemical Physics*, 2(13), 2999–3005. DOI: 10.1039/b0013811.

[25] Onda, A., Komatsu, T., Yashima, T. (2001). Preparation and catalytic properties of single-phase Ni-Sn intermetallic compound particles by CVD of Sn(CH3)4 onto Ni/silica. *Journal of Catalysis*, 201(1), 13–21. DOI: 10.1006/jcat.2001.3231.

[26] Shabaker, J.W., Huber, G.W., Dumesic, J.A. (2004). Aqueous-phase reforming of oxygenated hydrocarbons over Sn-modified Ni catalysts. *Journal of Catalysis*, 222(1), 180–191. DOI: 10.1016/j.jcat.2003.10.022.

[27] Huber, G.W., Shabaker, J.W., Dumesic, J.A. (2003). Raney Ni-Sn catalyst for H2 production from biomass-derived hydrocarbons. *Science*, 300(5628), 2075–2077. DOI: 10.1126/science.1085597.

[28] Marakatti, V.S., Arora, N., Rai, S., Sarma, S.C., Peter, S.C. (2018). Understanding the Role of Atomic Ordering in the Crystal Structures of NixSny toward Efficient Vapor Phase Furfural Hydrogenation. *ACS Sustainable Chemistry and Engineering*, 6(6), 7325–7338. DOI: 10.1021/acssuschemeng.7b04586.

[29] Petró, J., Bóta, A., László, K., Beyer, H., Kálmán, E., Dódony, I. (2000). A new alumina-supported, not pyrophoric Raney-type Ni-catalyst. *Applied Catalysis A: General*, 190(1–2), 73–86. DOI: 10.1016/S0926-860X(99)00267-7.

[30] Rodiansono, R., Astuti, M.D., Hara, T., Ichikuni, N., Shimazu, S. (2016). Efficient hydrogenation of levulinic acid in water using a supported Ni-Sn alloy on aluminium hydroxide catalysts. *Catalysis Science and Technology*, 6(9), 2955–2961. DOI: 10.1039/c5cy01731a.

[31] Rodiansono, R., Astuti, M.D., Mustikasari, K., Husain, S., Sutomo (2020). Recent progress in the direct synthesis of γ-valerolactone from biomass-derived sugars catalyzed by RANEY® Ni-Sn alloy supported on aluminium hydroxide. *Catalysis Science and Technology*, 10(22), 7768–7778. DOI: 10.1039/d0cy01356k.

[32] ICDD (1991). *International centre for diffraction data (ICDD).*

[33] Onda, A., Komatsu, T., Yashima, T. (1998). Preparation and catalytic properties of single phase Ni-Sn intermetallic compound particles by CVD of Sn(CH3)4 onto Ni/silica. *Chemical Communications*, (15), 1507–1508. DOI: 10.1039/a803071e.

[34] Agnelli, M., Louessard, P., el Mansour, A., Candy, J.P., Bournonville, J.P., Basset, J.M. (1989). Surface organometallic chemistry on metals preparation of new selective bimetallic catalysts by reaction of tetra-n-butyl tin with silica supported Rh, Ru and Ni. *Catalysis Today*, 6(1–2), 63–72. DOI: 10.1016/0920-5861(89)85007-2.

[35] Sweegers, C., Plomp, M., de Coninck, H.C., Meekes, H., van Enckevort, W.J.P., Hiralal, I.D.K., Rijkeboer, A. Surface topography of gibbsite crystals grown from aqueous sodium aluminate solutions. *Applied Surface Science*, 187(3–4), 218–234. DOI: 10.1016/S0169-4332(01)00995-3.

[36] Sweegers, C., de Coninck, H.C., Meekes, H., van Enckevort, W.J.P., Hiralal, I.D.K., Rijkeboer, A. (2001). Morphology, evolution and other characteristics of gibbsite crystals grown from pure and impure aqueous sodium aluminate solutions. Journal of Crystal Growth. 233(3), 567–582. DOI: 10.1016/S0022-0248(01)01615-3.

[37] Lefè, G., Fédoroff, M. (2002). Synthesis of bayerite (h-Al(OH)3) microrods by neutralization of aluminate ions at constant pH. *Materials Letters,* 56(6), 978–983. DOI: 10.1016/S0167-577X(02)00650-X.

[38] Sun, R., Zheng, M., Pang, J., Liu, X., Wang, J., Pan, X., Wang, A., Wang, X., Zhang, T. (2016). Selectivity-Switchable Conversion of Cellulose to Glycols over Ni–Sn Catalysts. *ACS Catalysis*, 6(1), 191–201. DOI: 10.1021/acscatal.5b01807.

[39] Nikolla, E., Schwank, J., Linic, S. (2007). Promotion of the long-term stability of reforming Ni catalysts by surface alloying. *Journal of Catalysis*, 250(1), 85–93. DOI: 10.1016/j.jcat.2007.04.020.

[40] Nikolla, E., Schwank, J., Linic, S. (2009). Comparative study of the kinetics of methane steam reforming on supported Ni and Sn/Ni alloy catalysts: The impact of the formation of Ni alloy on chemistry. *Journal of Catalysis*, 263(2), 220–227. DOI: 10.1016/j.jcat.2009.02.006.

[41] Sitthisa, S., Resasco, D.E. (2011). Hydrodeoxygenation of furfural over supported metal catalysts: A comparative study of Cu, Pd and Ni. *Catalysis Letters*, 141(6), 784–791. DOI: 10.1007/s10562-011-0581-7.

[42] Sitthisa, S., Pham, T., Prasomsri, T., Sooknoi, T., Mallinson, R.G., Resasco, D.E. (2011). Conversion of furfural and 2-methylpentanal on Pd/SiO2 and Pd-Cu/SiO2 catalysts. *Journal of Catalysis*, 280(1), 17–27. DOI: 10.1016/j.

[43] Pino, N., Sitthisa, S., Tan, Q., Souza, T., López, D., Resasco, D.E. (2017). Structure, activity, and selectivity of bimetallic Pd-Fe/SiO2 and Pd-Fe/Γ-Al2O3 catalysts for the conversion of furfural. *Journal of Catalysis*, 350, 30–40. DOI: 10.1016/j.jcat.2017.03.016.

[44] Maligal-Ganesh, R. v., Xiao, C., Goh, T.W., Wang, L.-L., Gustafson, J., Pei, Y., Qi, Z., Johnson, D.D., Zhang, S., Tao, F. (Feng), Huang, W. (2016). A Ship-in-a-Bottle Strategy To Synthesize Encapsulated Intermetallic Nanoparticle Catalysts: Exemplified for Furfural Hydrogenation. *ACS Catalysis*, 6(3), 1754–1763. DOI: 10.1021/acscatal.5b02281.

[45] Rodiansono, R., Astuti, M.D., Ghofur, A., Sembiring, K.C. (2015). Catalytic hydrogenation of levulinic acid in water into γ-valerolactone over bulk structure of inexpensive intermetallic Ni-Sn alloy catalysts. *Bulletin of Chemical Reaction Engineering & Catalysis*, 10(2), 192–200. DOI: 10.9767/bcrec.10.2.8284.192-200.

[46] Komatsu, T., Onda, A. (2008). Catalytic properties of single-phase intermetallic compounds. *Catalysis Surveys from Asia*, 12(1), 6–15. DOI: 10.1007/s10563-007-9031-3.

[47] Onda, A., Komatsu, T., Yashima, T. (2004). Characterizations and catalytic properties of fine particles of Ni-Sn intermetallic compounds supported on SiO_2. *Journal of Catalysis*, 221(2), 378–385. DOI: 10.1016/j.jcat.2003.08.012.

[48] Marinelli, T.B.L.W., Ponec, V. (1995). A Study on the Selectivity in Acrolein Hydrogenation on Platinum Catalysts: A Model for Hydrogenation of α,ß-Unsaturated Aldehydes. *Journal of Catalysis*, 156(1), 51–59. DOI: 10.1006/jcat.1995.1230.

[49] Studt, F., Abild-Pedersen, F., Bligaard, T., Sørensen, R.Z., Christensen, C.H., Nørskov, J.K. (2008). Identification of non-precious metal alloy catalysts for selective hydrogenation of acetylene. *Science*, 320(5881), 1320–1322. DOI: 10.1126/science.1156660.